13

On breathing motion compensation in myocardial perfusion imaging

Gert Wollny[1,2], María J. Ledesma-Carbayo[1,2], Peter Kellman[3] and Andrés Santos[1,2]
[1]*Biomedical Image Technologies, Department of Electronic Engineering, ETSIT, Universidad Politécnica de Madrid, Spain*
[2]*Ciber BNN, Spain,*
[3]*Laboratory of Cardiac Energetics, National Heart, Lung and Blood Institute, NIH, DHHS, Bethesda, MD USA*

1. Introduction

First-pass gadolinium enhanced, myocardial perfusion *magnetic resonance imaging* (MRI) can be used to observe and quantify blood flow to the different regions of the myocardium. Ultimately such observation can lead to diagnosis of coronary artery disease that causes narrowing of these arteries leading to reduced blood flow to the heart muscle.
A typical imaging sequence includes a pre-contrast baseline image, the full cycle of contrast agent first entering the right heart ventricle (RV), then the left ventricle (LV), and finally, the agent perfusing into the LV myocardium (Fig. 1). Images are acquired to cover the full first pass (typically 60 heartbeats) which is too long for the patient to hold their breath. Therefore, a non-rigid respiratory motion is introduced into the image sequence which results in a misalignment of the sequence of images through the whole acquisition. For the automatic analysis of the sequence, a proper alignment of the heart structures over the whole sequence is desired.

1.1 State of the art

The mayor challenge in the motion compensation of the contrast enhanced perfusion imaging is that the contrast and intensity of the images change locally over time, especially in the region of interest, the left ventricular myocardium. In addition, although the triggered imaging of the heart results in a more-or-less rigid representation of the heart, the breathing movement occurs locally with respect to the imaged area, yielding non-rigid deformations within the image series. Various registration methods have been proposed to achieve an alignment of the myocardium. For example, Delzescaux et al. (Delzescaux et al., 2003) proposed a semi-automated approach to eliminate the motion and avoid the problems of intensity change and non-rigid motion: An operator selects manually the image with the highest gradient magnitude, from which several models of heart structures were created as a reference. By using potential maps and gradients they eliminated the influence of the intensity change and restricted the processing to the heart region. Registration was then achieved through translation only.

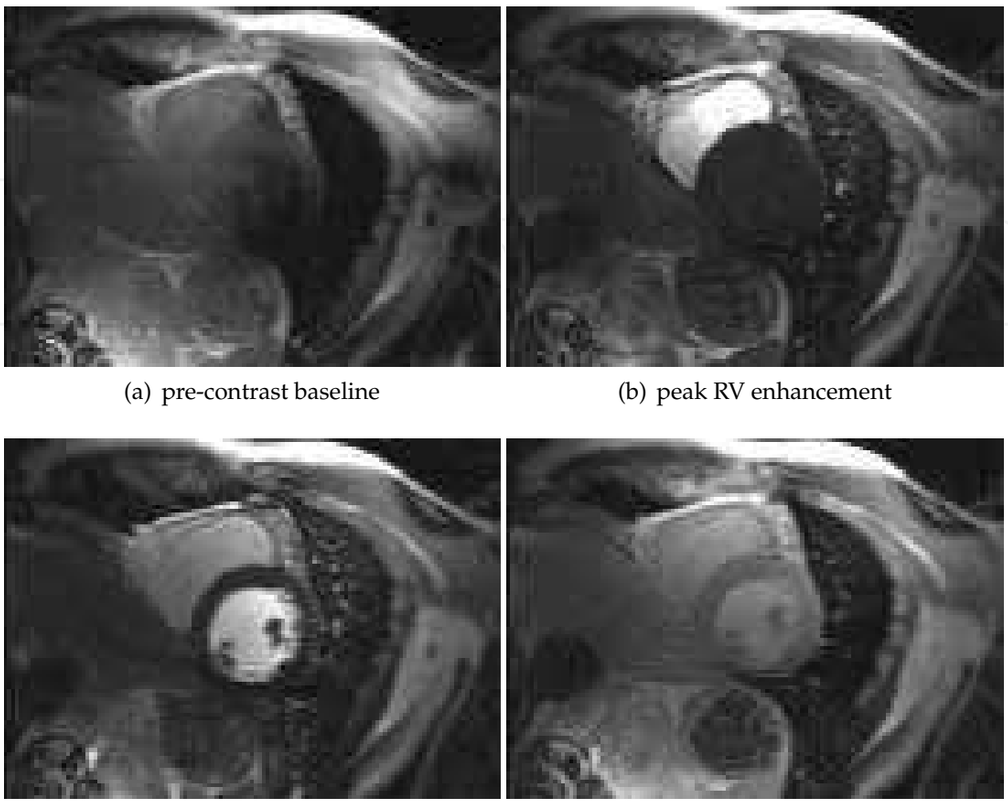

(a) pre-contrast baseline (b) peak RV enhancement

(c) peak LV enhancement (d) peak myocardial enhancement

Fig. 1. Images from a first-pass gadolinium enhanced, myocardial perfusion MRI of a patient with chronic myocardial infarction (MI).

In (Dornier et al., 2003) two methods where described that would either use simple rectangular masks around the myocardium or an optimal masks, where the area with the high intensity change where eliminated as well. Rigid registration was then achieved by employing a spline-based multi-resolution scheme and optimizing the sum of squared differences. They reported, that using an optimal mask yields results that are comparable to gold standard data set measurements, whereas using the rectangular mask did not show improvements over values obtained from the raw images. A two step registration approach was introduced by (Gupta et al., 2003), the first step comprising the creation of a binary mask of the target area in all images obtaining an initial registration by aligning their centers of mass. Then, in the second step, they restricted the evaluation of the registration criterion to a region around the center of mass, and thereby, to the rigidly represented LV myocardium. By optimizing the cross-correlation of the intensities, complications due to the intensity change were avoided and rigid registration achieved.

Others measures that are robust regarding differences in the intensity distribution can be drawn from Information Theory. One such measure is, e.g. *Normalized Mutual Information*(NMI) (Studholme et al., 1999). Wong et al. (Wong et al., 2008) reported its successful use to achieve rigid motion compensation if the evaluation of the registration criterion was

restricted to the LV by a rectangular mask. One more sophisticated approach to overcome the problems with the local intensity change was presented by Milles et al. (Milles et al., 2007). They proposed to identify three images (base-line, peak RV enhancement, peak LV enhancement) by using Independent Component Analysis (ICA) of the intensity curve within the left and the right ventricle. These three images then form a vector base that is used to create a reference image for each time step by a weighted linear combination, hopefully exhibiting a similar intensity distribution like the according original image to be registered. Image registration of the original image to the composed reference image is then achieved by a rigid transformation minimizing the Sum of Squared Differences (SSD). Since the motion may also affect the ICA base images, this approach was later extended to run the registration in two passes (Milles et al., 2008).
Since rigid registration requires the use of some kind of mask or feature extraction to restrict the alignment process to the near-rigid part of the movement, and, since non-rigid deformations are not taken into account by these movements other authors target for non-rigid registration. One such example was presented in (Ólafsdóttir, 2005): All images were registered to the last image in the series were the intensities have settled after the contrast agent passed through the ventricles and the myocardium, and non-rigid registration was done by using a B-spline based transformation model and optimizing NMI. However, the evaluation of NMI is quite expensive in computational terms, and, as NMI is a global measure, it might not properly account for the local intensity changes.
Some other methods for motion compensation in cardiac imaging have been reported in the reviews in (Makela et al., 2002) and (Milles et al., 2008).

1.2 Our contribution

In order to compensate for the breathing movements, we use non-rigid registration, and to avoid the difficulties in registration induced by the local contrast change, we follow Haber and Modersitzki (Haber & Modersitzki, 2005) using a modified version of their proposed image similarity measure that is based on *Normalized Gradient Fields* (NGF). Since this cost function does not induce any forces in homogeneous regions of the chosen reference image, we combine the NGF based measure with SSD. In addition, we use a serial registration procedure, where only images are registered that follow in temporal succession, reducing the influence of the local contrast change further. The remainder of this chapter first discusses non-rigid registration, then, we focus on the NGF based cost measure and our modifications to it as well as combining the new measure with the well known SSD measure. We give some pointers about the validation of the registration, and finally, we present and discuss the results and their validation.

2. Methods

2.1 Image registration

Image registration can be defined as follows: consider an image domain $\Omega \subset \mathbb{R}^d$ in the d-dimensional Euclidean space and an intensity range $\mathbb{V} \subset \mathbb{R}$, a moving image $M : \Omega \to \mathbb{V}$, a reference image $R : \Omega \to \mathbb{V}$, a domain of transformations $\Theta := \{T : \Omega \to \Omega\}$, and the notation $M_T(\mathbf{x}) := M(T(\mathbf{x}))$, or short $M_T := M(T)$. Then, the registration of M to R aims at finding a transformation $T_{\text{reg}} \in \Theta$ according to

$$T_{\text{reg}} := \min_{T \in \Theta} \left(F(M_T, R) + \kappa E(T) \right). \tag{1}$$

F measures the similarity between the (transformed) moving image M_T and the reference, E ensures a steady and smooth transformation T, and κ is a weighting factor between smoothness and similarity. With non-rigid registration, the domain of possible transformations Θ is only restricted to be neighborhood-preserving. In our application, the F is derived from a so called voxel-similarity measure that takes into account the intensities of the whole image domain. In consequence, the driving force of the registration will be calculated directly from the given image data.

2.1.1 Image similarity measures

Due to the contrast agent, the images of a perfusion study exhibit a strong local change of intensity. A similarity measure used to register these images should, therefore, be of a local nature. One example of such measure are Normalized Gradient Fields (NGF) as proposed in (Haber & Modersitzki, 2005).

Given an image $I(\mathbf{x}) : \Omega \to \mathbb{V}$ and its noise level η, a measure ϵ for boundary "jumps" (locations with a high gradient) can be defined as

$$\epsilon := \eta \frac{\int_\Omega |\nabla I(\mathbf{x})| d\mathbf{x}}{\int_\Omega d\mathbf{x}}, \tag{2}$$

and with

$$\|\nabla I(\mathbf{x})\|_\epsilon := \sqrt{\sum_{i=1}^{d} (\nabla I(\mathbf{x}))_i^2 + \epsilon^2}, \tag{3}$$

the NGF of an image I is defined as follows:

$$\mathbf{n}_\epsilon(I, \mathbf{x}) := \frac{\nabla I(\mathbf{x})}{\|\nabla I(\mathbf{x})\|_\epsilon}. \tag{4}$$

In (Haber & Modersitzki, 2005), two NGF based similarity measures where defined,

$$F_{\mathrm{NGF}}^{(\cdot)}(M, R) := -\frac{1}{2} \int_\Omega \|\mathbf{n}_\epsilon(R, \mathbf{x}) \cdot \mathbf{n}_\epsilon(M, \mathbf{x})\|^2 d\mathbf{x} \tag{5}$$

$$F_{\mathrm{NGF}}^{(\times)}(M, R) := \frac{1}{2} \int_\Omega \|\mathbf{n}_\epsilon(R, \mathbf{x}) \times \mathbf{n}_\epsilon(M, \mathbf{x})\|^2 d\mathbf{x} \tag{6}$$

and successfully used for rigid registration. However, as discussed in (Wollny et al., 2008) for non-rigid registration, these measures resulted in poor registration: (5) proved to be numerically unstable resulting in a non-zero gradient even in the optimal case $M = R$, and (6) is also minimized, when the gradients in both images do not overlap at all. Therefore, we define another NGF based similarity measure:

$$F_{\mathrm{NGF}}(M, R) := \frac{1}{2} \int_\Omega \|(\mathbf{n}_\epsilon(M) - \mathbf{n}_\epsilon(R)) \cdot \mathbf{n}_\epsilon(R)\|^2 d\mathbf{x}. \tag{7}$$

This cost function needs to be minimized, is always differentiable and its evaluation as well as the evaluation of its derivatives are straightforward, making it easy to use it for non-rigid registration. In the optimal case, $M = R$ the cost function and its first order derivatives are zero and the evaluation is numerically stable. $F_{\mathrm{NGF}}(\mathbf{x})$ is minimized when $\mathbf{n}_\epsilon(R, \mathbf{x}) and \mathbf{n}_\epsilon(M, \mathbf{x})$ are parallel and point in the same direction and even zero when $\mathbf{n}_\epsilon(R, \mathbf{x})(\mathbf{x})$ and $\mathbf{n}_\epsilon(M, \mathbf{x})(\mathbf{x})$ have the same norm. However, the measure is also zero when $\mathbf{n}_\epsilon(R, \mathbf{x})$ has zero norm, i.e.

in homogeneous areas of the reference image. This requires some additional thoughts when good non-rigid registration is to be achieved. For that reason we also considered to use a combination of this NGF based measure (7) with the Sum of Squared Differences (SSD)

$$F_{\mathrm{SSD}}(M,R) := \frac{1}{2}\int_{\Omega}\left(M(\mathbf{x}) - R(\mathbf{x})\right)^2 d\mathbf{x} \tag{8}$$

as registration criterion. This combined cost function will be defined as

$$F_{\mathrm{Sum}} := \alpha F_{\mathrm{NGF}} + \beta F_{\mathrm{SSD}} \tag{9}$$

with α and β weighting between the two parts of the cost functions.

2.1.2 Regularization, transformation space and optimization

Two measures are taken to ensure a smooth transformation: On one hand, the transformation is formulated in terms of uniform B-splines (Kybic & Unser, 2003),

$$T(x) := \sum_{i=0}^{(m-D)} P_i \beta_{i,D}(x - x_i) \tag{10}$$

with the control points P_i, the spline basis functions $\beta_{i,D}$ of dimension D, knots x_i , and a uniform knots spacing $h := x_i - x_{i-1} \forall i$. The smoothness of the transformation can be adjusted by the knot spacing h.
On the other hand, our registration method uses a Laplacian regularization (Sánchez Sorzano et al., 2005),

$$E_{\mathrm{L}}(T) := \int_{\Omega}\sum_{i}^{d}\sum_{j}^{d}\left\|\frac{\partial^2}{\partial x_i \partial x_j}T(\mathbf{x})\right\|^2 d\mathbf{x}. \tag{11}$$

As given in eq. (1) the latter constraint will be weighted against the similarity measure by a factor κ. To solve the registration problem by optimizing (1), generally every gradient based optimizer could be used. We employed a variant of the Levenberg-Marquardt optimizer (Marquardt, 1963) that will optimize a predefined number of parameters during each iteration which are selected based on the magnitude of the cost function gradient.

2.2 Serial registration

As the result of the myocardic perfusion imaging over N time steps $\mathfrak{S} := \{1, 2, ..., N\}$, a series of N images $\mathfrak{J} := \{I_i : \Omega \to \mathbb{V} | i \in \mathfrak{S}\}$ is obtained. In order to reduce the influence of the changing intensities, a registration of all frames to one reference frame has been rules out and replaced by a serial registration. In order to be able to choose a reference frame easily, the following procedure is applied: For each pair of subsequent images (I_i, I_{i+1}) registration is done twice, one selecting the earlier image of the series as a reference (backward registration), and the second by using the later image as the reference (forward registration). Therefore, for each pair of subsequent images I_i and I_{i+1}, a forward transformation $T^{i,i+1}$ and a backward transformation $T^{i+1,i}$ is obtained. Now, consider the concatenation of two transformations

$$T_a(T_b(\mathbf{x})) := (T_b \oplus T_a)(\mathbf{x}); \tag{12}$$

in order to align all image of the series, a reference frame i_{ref} is chosen, and all other images I_i are deformed to obtain the corresponding aligned image $I_i^{(\text{align})}$ by applying the subsequent forward or backward transformations

$$I_i^{(\text{align})} := \begin{cases} I_i\left(\bigoplus_{k=i_{\text{ref}}}^{i+1} T^{k,k-1}(\mathbf{x})\right) & \text{if } i < i_{\text{ref}}, \\ I_i\left(\bigoplus_{k=i_{\text{ref}}}^{i-1} T^{k,k+1}(\mathbf{x})\right) & \text{if } i > i_{\text{ref}}, \\ I_{i_{\text{ref}}} & \text{otherwise.} \end{cases} \tag{13}$$

In order to minimize the accumulation of errors for a series of n images one would usually choose $i_{\text{ref}} = \lfloor \frac{n}{2} \rfloor$ as the reference frame. Nevertheless, with the full set of forward and backward transformations at hand, any reference frame can be chosen.

2.3 Towards validation

In our validation, we focus on comparing perfusion profiles obtained from the registered image series to manually obtained perfusion profiles, because these profiles are the final result of the perfusion analysis and their accuracy is of most interest. To do so, in all images the myocardium of the left ventricle was segmented manually into six segments $\mathbb{S} = \{S_1, S_2, ..., S_6\}$ (Fig. 2).

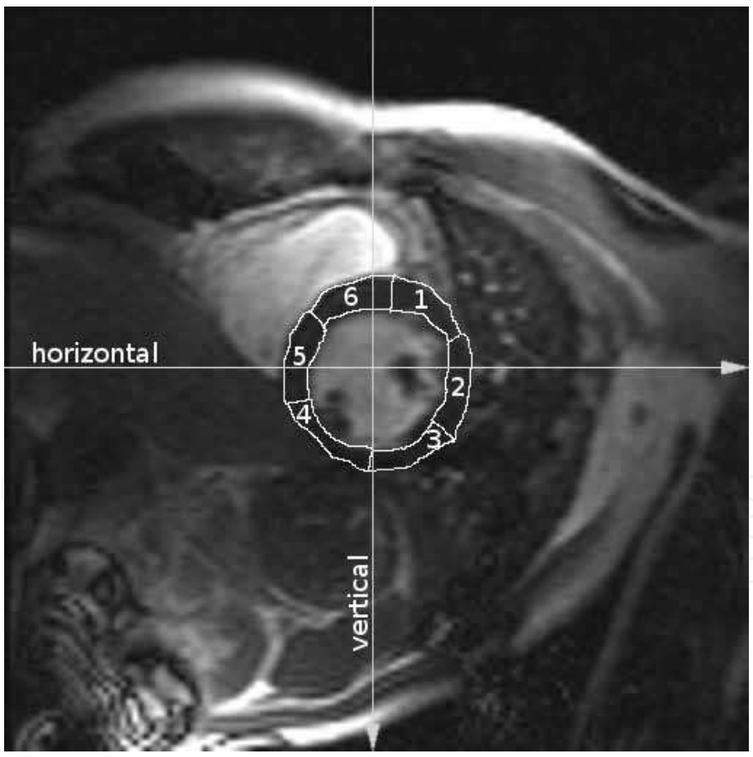

Fig. 2. Segmentation of the LV myocardium into six regions and horizontal as well as vertical profiles of the original image series.

The hand segmented reference intensity profiles $P_{\text{hand}}^{(s)}$ of the sections $s \in \mathbb{S}$ over the image series were obtained by evaluating the average intensities in these regions and plotting those

over the time of the sequence (e.g. Fig. 4). By using only the segmentation of the reference image I_{ref} as a mask to evaluate the intensities in all registered images, the registered intensity profiles $P^{(s)}_{\text{reg}}$ were obtained. Likewise, the intensity profiles $P^{(s)}_{\text{org}}$ for the unregistered, original series were evaluated based on the unregistered images.
In order to make it possible to average the sequences of different image series for a statistical analysis, the intensity curves K were normalized based on the reference intensity range $[v_{\min}, v_{\max}]$, with $v_{\min} := \min_{s\in\mathfrak{S},t\in\mathfrak{S}} P^{(s)}_{\text{hand}}(t)$ and $v_{\max} := \max_{s\in\mathfrak{S},t\in\mathfrak{S}} P^{(s)}_{\text{hand}}(t)$ by using

$$\hat{P} := \left\{ \frac{v - v_{\min}}{v_{\max} - v_{\min}} \middle| \, v \in P \right\}. \tag{14}$$

To quantify the effect of the motion compensation, the quotient of the sum of the distance between registered and reference curve as well as the sum of the distance between unregistered and reference curve are evaluated, resulting in the value Q_s as quality measure for the registration of section s:

$$Q_S := \frac{\sum_{t\in\mathfrak{S}} |\hat{P}^{(s)}_{\text{reg}}(t) - \hat{P}^{(s)}_{\text{hand}}(t)|}{\sum_{t\in\mathfrak{S}} |\hat{P}^{(s)}_{\text{org}}(t) - \hat{P}^{(s)}_{\text{hand}}(t)|} \tag{15}$$

As a result $Q_s > 0$ and smaller values of Q_s will express better registration.
As a second measure, we also evaluated the squared Pearson correlation coefficient R^2 of the manually estimated profiles and the unregistered respective the registration profiles. The range of this coefficient is $R^2 \in [0, 1]$ with higher values indicating a better correlation between the data sets. Since the correlation describes the quality of linear dependencies, it doesn't account for an error in scaling or an intensity shift. Finally, we consider the standard deviation of the intensity in the six sections S_i of the myocardium $\sigma_{s_i,t}$ for each time step $t \in \mathfrak{S}$. Since the intensity in these regions is relatively homogeneous, only noise and the intensity differences due to disease should influence this value. Especially, in the first part of the perfusion image series, when the contrast agent passes through the right and left ventricle, this approach makes it possible to assess the registration quality without comparing it to a manual segmentation: Any mis-alignment between the section mask of the reference image and the corresponding section of the analyzed series frame will add pixels of the interior of the ventricles to one or more of the sections, increasing the intensity range, and hence its standard deviation. With proper alignment, on the other hand, this value will decrease.

3. Experiments and results

3.1 Experiments

First pass contrast enhanced myocardial perfusion imaging data was acquired during free-breathing using 2 distinct pulse sequences: a hybrid GRE-EPI sequence and a trueFISP sequence. Both sequences were ECG triggered and used 90 degree saturation recovery imaging of several slices per R-R interval acquired for 60 heartbeats. The pulse sequence parameters for the true-FISP sequence were 50 degree readout flip angle, 975 Hz/pixel bandwidth, TE/TR/TI= 1.3/2.8/90 ms, 128x88 matrix, 6mm slice thickness; the GRE-EPI sequence parameters were: 25 degree readout flip angle, echo train length = 4, 1500 Hz/pixel bandwidth, TE/TR/TI=1.1/6.5/70 ms, 128x96 matrix, 8 mm slice thickness. The spatial resolution was approximately 2.8mm x 3.5mm. Parallel imaging using the TSENSE method with acceleration factor = 2 was used to improve temporal resolution and spatial coverage. A single dose of contrast agent (Gd-DTPA, 0.1 mmol/kg) was administered at 5 ml/s, followed by saline

flush. Motion compensation was performed for seven distinct slices of two patient data sets covering different levels of the LV-myocardium. All in all we analyzed 17 slices from six different patients, three breathing freely, one holding his breath during the first half of the sequence, and breathing with two deep gasps in the second half, and two breathing shallow.
The registration software was implemented in C++, the registration procedure used B-Splines of degree 2 and varying parameters for the number $l \in \{1, 2, 3\}$ of multi-resolution levels, the knot spacing $h \in \{14, 16, 20\}$ pixels for the B-Spline coefficients, and the weight $\kappa \in \{0.8, 1.0, 2.0, 3.0\}$ of the Laplacian regularization term. Estimating the noise level of images is a difficult problem, we approximated η by $\sigma(\nabla I)$ standard deviation of the intensity gradient.

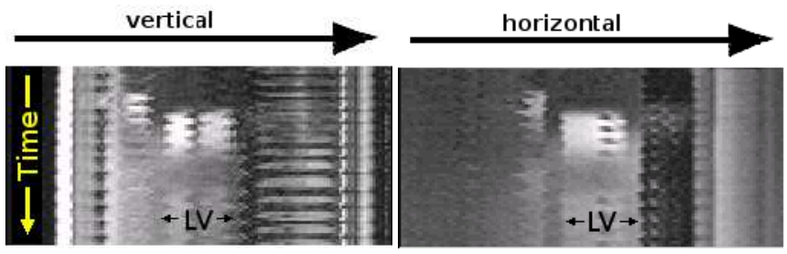

(a) Original image series

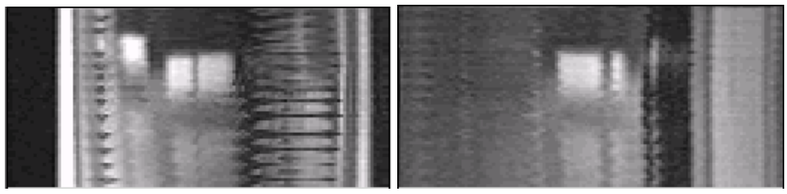

(b) Registration using NGF only, $\kappa = 1.0$, note the bad alignment and the drift in the second (lower) half of the series

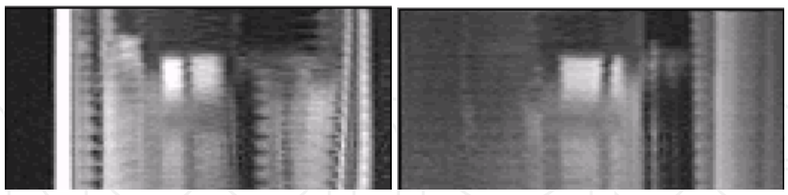

(c) Registration using NGF + 0.1 SSD, $\kappa = 2.0$, the drift vanished and alignment is in general better then with NGF only

Fig. 3. Registration result by using $l = 3$ multi-resolution levels, and a knot spacing $h = 16mm$. Left: vertical cut, right: horizontal cut.

To ensure registration driving forces exist over the whole image domain, we also run experiments with the combined cost function (9), setting $\alpha = 1.0$ and $\beta \in 0.1, 0.5, 1.0$. Since all images are of the same modality, we expect that combining the two measures will yield the same or better results. Tests showed that applying F_{SSD} as only registration criterion doesn't yield usable results.

3.2 Registration results

Fully automatic alignment of a series of 60 images, including 118 image-to-image registrations at the full resolution of size 196x256 pixels and the transformation of the images to the reference frame 30, was achieved in approximately 5 minutes running the software on a Linux workstation (Intel(R) Core(TM)2 CPU 6600). This time could be further reduced if a bounding box were to be applied and by exploiting the multi-core architecture of the processing and running the registrations in parallel.

First, the quality of the registration was assessed visually observing videos as well as horizontal and vertical profiles through the time-series stack. An example of the profiles location is given in Fig. 2.

In terms of the validation measure, we obtained the best results using $l = 3$ multi-resolution levels and a knot-spacing of $h = 16$ pixels in each spacial direction. For the registration using NGF, a regularizer weight $\kappa = 1.0$ yielded best results, whereas for the combination of NGF and SSD $\kappa = 2.0$ was best. The registration by using F_{NGF} yields good results for the first half of the sequence, where the intensity contrast is higher, and the gradients are, therefore, stronger. In the second half, the sequential registration resulted in a bad alignment and a certain drift of the left ventricle (Fig. 3 (b)).

Combining F_{NGF} and F_{SSD} results in a significant improvement of the alignment for the second part of the sequence (Fig. 3 (c)) and provided similar results for the first half. Best results where obtained for $\beta = 0.5$. Following this scheme, a good reduction of the breathing motion was achieved in all of the analyzed slices.

The registration procedure performed equally well for all types of patient data - freely breathing, shallow breathing, and partial breath holding. It has to be noted though, that for some slices the registration didn't perform very well, resulting in errors that are then propagated through the far part of the series as seen from the reference point.

For the validation, the intensity curves before and after registration were obtained and compared to manually segmented ones (Fig. 4). In most cases, the intensity curves after registration resemble manual obtained ones very well, correlation between the two curves increased considerably 1.

		Mean	SD	Median	Min	Max
Q_S smaller is better		0.68	0.42	0.55	0.16	2.72
R^2 larger is better	unregistered	0.87	0.16	0.93	0.02	1.00
	registered	0.97	0.05	0.99	0.61	1.00
$\sigma_{*,*}$ smaller is better	unregistered	0.63	0.54	0.51	0.05	8.99
	registered	0.50	0.33	0.44	0.03	4.01
	segmented	0.46	0.22	0.41	0.04	1.30

Table 1. The registration quality Q_s, correlation R^2, and section intensity variation σ for the optimal parameters as given in the text.

The average and median of the quality measure Q_s support the findings of a generally good motion compensation, as do the improved correlation R^2 between the intensity profiles and the reduced intensity variations in the myocardium sections $\sigma_{*,*}$.

However, the maxima of Q_s above 1.0 indicate that in some cases motion compensation is not, or only partially achieved. For our experiments, which included 17 distinct slices and, hence, 102 myocardium sections, registration failed partially for 16 sections. This is mostly due to

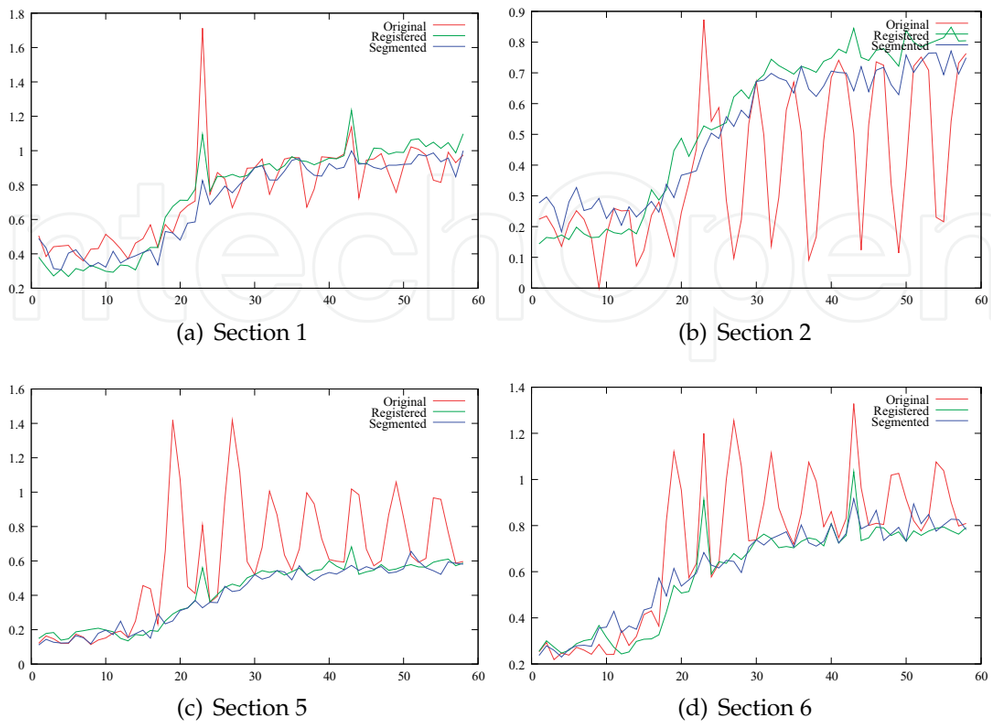

(a) Section 1 (b) Section 2

(c) Section 5 (d) Section 6

Fig. 4. Intensity curves before and after registration compared to the manually obtained ones. The alignment was evaluated by using frame 30 as reference. Note the periodic intensity change in the unregistered series that results from the breathing movement, and how well the registered series resembles the manually obtained intensity curve.

the serial registration procedure, where one failed registration of an image pair will propagate and small registration errors might accumulate when the final deformation is evaluated according to (13) and with respect to a certain reference image $I_{i_{\text{ref}}}$. In Fig. 5, these problems are illustrated: The registration of two frames, namely 13 and 14 in one of the analyzed series failed, resulting in partial misalignment of all images on the far side of this image pair with respect to the reference frame. For one section of the myocardium, this resulted in large errors for most of the first 13 frames in its intensity profile (Fig. 5(a)) which is also reflected by an increase of the standard deviation (Fig. 5(b)). In the second half of the series, registration errors accumulate, resulting in an ever increasing deviation of the intensity profile obtained by hand segmentation.

Note however, if only a part of the intensity profile is of interest, it is possible to minimize this accumulation of errors by selecting a proper reference frame and reducing the analysis to the part of the intensity profile. In the above example (Fig. 5), by restricting evaluation to the frames 15-35, and thereby, focusing on the upslope, it is shown that the registration quality is sufficient to analyze this part of the perfusion process, although a complete registration could not be achieved. This can be expressed in terms of the registration quality Q_s, which is greater than 1.0 in section 3 for two distinct reference frames when analyzing the full series, but smaller in the sub-range (Table 2).

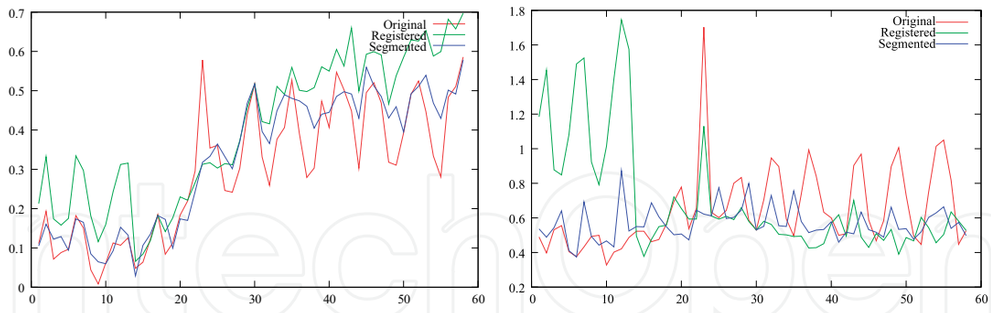

(a) Profiles (b) Intensity deviation

Fig. 5. In this intensity profile (a) the accumulation of registration errors is apparent which are in part reflected by the increased standard deviation (b).

Q_s (smaller is better)	Sections of the myocardium					
	1	2	3	4	5	6
full series, reference 30	0.88	0.42	1.52	0.31	0.17	0.29
full series, reference 25	0.77	0.35	1.07	0.38	0.18	0.36
frames 15-35, reference 30	0.80	0.31	0.56	0.22	0.12	0.23
frames 15-35, reference 25	0.48	0.24	0.29	0.26	0.12	0.34

Table 2. The registration quality Q, of a whole example series versus a part of it. Note, the dependence of the quality from the reference frame and the significantly better registration quality of the subset compared to the whole series.

4. Conclusion

In this work, we proposed a new scheme for breathing motion compensation in MRI perfusion studies based on non-rigid registration. In order to reduce the influence of the change of intensity, which is induced by the contrast agent as it passes through the both heart ventricles and the myocardium, we used a serial registration scheme where only subsequent images of the series are registered. In addition, we have introduced a new image similarity measure that is based on normalized gradient fields and was improved over the previous proposal in (Haber & Modersitzki, 2005). This measure is of a very local nature, and therefore, well suited to obtain non-rigid registration for images with local contrast change, as it is the case in myocardial perfusion MRI. Our experiments show that using this measure alone yields a good registration only for the images of the series that exhibit a high contrast and, hence, strong gradients in the regions of interest. When the intensity contrast is low, small registration errors may occur and, because of the serial registration scheme, these errors accumulate resulting an increasing misalignment over the series time course.

We were able to improve these results by combining the normalized gradient field based cost function with the sum of squared differences, so that the first would take precedence in regions with high contrast and, hence, strong gradients, while the latter ensures a steady registration in areas with low contrast and, therefore, small gradients.

The serial registration approach results in a high dependency on a good registration of all neighboring image pairs, if one is to obtain a good registration of the whole image series.

In addition, all over registration quality may vary depending on the reference frame chosen. However, for an analysis of only a part of the series, it is possible to reduce the influence of accumulating errors by selecting a reference close or within the time frame of interest resulting in sufficiently good registration.

5. ACKNOWLEDGMENTS

This study was partially supported by research projects TIN2007-68048-C02-01, CDTI-CDTEAM and SINBAD (PS-010000-2008-1) from SpainŠs Ministry of Science and Innovation.

6. References

Delzescaux, T., Frouin, F., Cesare, A. D., Philipp-Foliguet, S., Todd-Pokropek, A., Herment, A. & Janier, M. (2003). Using an adaptive semiautomated self-evaluated registration technique to analyze mri data for myocardial perfusion assessment, *J. Magn. Reson. Imaging* **18**: 681âĂŞ 690.

Dornier, C., Ivancevic, M., Thevenaz, P. & Vallee, J.-P. (2003). Improvement in the quantification of myocardial perfusion using an automatic spline-based registration algorithm, *J. Magn. Reson. Imaging* **18**: 160–168.

Gupta, S., Solaiyappan, M., Beache, G., Arai, A. E. & Foo, T. K. (2003). Fast method for correcting image misregistration due to organ motion in time-series mri data, *Magnetic Resonance in Medicine* **49**: 506 âĂŞ514.

Haber, E. & Modersitzki, J. (2005). Beyond mutual information: A simple and robust alternative, *in* A. H. Hans-Peter Meinzer, Heinz Handels & T. Tolxdorff (eds), *Bildverarbeitung für die Medizin 2005*, Informatik Aktuell, Springer Berlin Heidelberg, pp. 350–354.

Kybic, J. & Unser, M. (2003). Fast parametric elastic image registration, *IEEE Transactions on Image Processing* **12**(11): 1427–1442.

Makela, T., Clarysse, P., Sipila, O., Pauna, N., Pham, Q., Katila, T. & Magnin, I. (2002). A review of cardiac image registration methods, *IEEE Transactions on Medical Imaging* **21**(9): 1011–1021.

Marquardt, D. (1963). An Algorithm for Least-Squares Estimation of Nonlinear Parameters, *SIAM J. Appl. Math.* **11**: 431–441.

Milles, J., van der Geest, R. J., Jerosch-Herold, M., Reiber, J. H. & Lelieveldt, B. P. (2007). Fully automated registration of first-pass myocardial perfusion MRI using independent component analysis., *Inf Process Med Imaging* **20**: 544–55.

Milles, J., van der Geest, R., Jerosch-Herold, M., Reiber, J. & Lelieveldt, B. (2008). Fully automated motion correction in first-pass myocardial perfusion mr image sequences, *Medical Imaging, IEEE Transactions on* **27**(11): 1611–1621.

Ólafsdóttir, H. (2005). Nonrigid registration of myocardial perfusion MRI, *Proc. Svenska Symposium i Bildanalys, SSBA 2005, Malmø, Sweden*, SSBA. `http://www2.imm.dtu.dk/pubdb/p.php?3599`.

Sánchez Sorzano, C., Thévenaz, P. & Unser, M. (2005). Elastic registration of biological images using vector-spline regularization, *IEEE Transactions on Biomedical Engineering* **52**(4): 652–663.

Studholme, C., Hawkes, D. J. & Hill, D. L. G. (1999). An overlap invariant entropy measure of 3d medical image alignment, *Pattern Recognition* **32**(1): 71–86.

Wollny, G., Ledesma-Carbayo, M. J., Kellman, P. & Santos, A. (2008). A New Similarity Measure for Non-Rigid Breathing Motion Compensation of Myocardial Perfusion MRI, *Proc. of the 30th Int. Conf. of the IEEE Eng. in Medicine and Biology Society*, Vancouver, BC, Canada, pp. 3389–3392.

Wong, K., Yang, E., Wu, E., Tse, H.-F. & Wong, S. T. (2008). First-pass myocardial perfusion image registration by maximization of normalized mutual information, *J. Magn. Reson. Imaging* **27**: 529–537.

IntechOpen

New Developments in Biomedical Engineering
Edited by Domenico Campolo

ISBN 978-953-7619-57-2
Hard cover, 714 pages
Publisher InTech
Published online 01, January, 2010
Published in print edition January, 2010

Biomedical Engineering is a highly interdisciplinary and well established discipline spanning across engineering, medicine and biology. A single definition of Biomedical Engineering is hardly unanimously accepted but it is often easier to identify what activities are included in it. This volume collects works on recent advances in Biomedical Engineering and provides a bird-view on a very broad field, ranging from purely theoretical frameworks to clinical applications and from diagnosis to treatment.

How to reference
In order to correctly reference this scholarly work, feel free to copy and paste the following:

Gert Wollny, Maria J. Ledesma-Carbayo, Peter Kellman and Andres Santos (2010). On Breathing Motion Compensation in Myocardial Perfusion Imaging, New Developments in Biomedical Engineering, Domenico Campolo (Ed.), ISBN: 978-953-7619-57-2, InTech, Available from: http://www.intechopen.com/books/new-developments-in-biomedical-engineering/on-breathing-motion-compensation-in-myocardial-perfusion-imaging

INTECH
open science | open minds

InTech Europe
University Campus STeP Ri
Slavka Krautzeka 83/A
51000 Rijeka, Croatia
Phone: +385 (51) 770 447
Fax: +385 (51) 686 166
www.intechopen.com

InTech China
Unit 405, Office Block, Hotel Equatorial Shanghai
No.65, Yan An Road (West), Shanghai, 200040, China
中国上海市延安西路65号上海国际贵都大饭店办公楼405单元
Phone: +86-21-62489820
Fax: +86-21-62489821

IntechOpen